Journal of Photochemistry and Photobiology A: Chemistry 210 (2010) 200–208

Contents lists available at ScienceDirect

Journal of Photochemistry and Photobiology A: Chemistry

journal homepage: www.elsevier.com/locate/jphotochem

Photophysical properties of newly synthesized fluorinated zinc phthalocyanines in the presence of CdTe quantum dots and the accompanying energy transfer processes

Ali Erdoğmuş[a,b], Sharon Moeno[a], Christian Litwinski[a], Tebello Nyokong[a,*]

[a] Department of Chemistry, Rhodes University, Grahamstown 6140, South Africa
[b] Department of Chemistry, Yildiz Technical University, 34210 Esenler, Istanbul, Turkey

ARTICLE INFO

Article history:
Received 21 September 2009
Received in revised form 7 December 2009
Accepted 15 December 2009
Available online 23 December 2009

Keywords:
Zinc phthalocyanine
Quantum dots
Mercaptopropionic acid
Förster resonance energy transfer

ABSTRACT

The photophysical properties of two newly synthesized phthalocyanines (Pcs) were studied in the presence and the absence of 3-mercaptopropionic acid (MPA) capped quantum dots (QDs). Energy transfer processes resulting from the combination of QDs and the Pcs: 4-(tetrakis-5-(trifluoromethyl)-2-mercaptopyridinephthalocyaninato)zinc(II) (TtfmMPyZnPc, **3**) and 4-(tetrakis-5-(trifluoromethyl)-2-pyridyloxyphthalocyaninato) zinc(II) (TtfmPyZnPc, **4**) were also studied. The photophysical properties of the Pcs in the presence of QDs were enhanced and Förster resonance energy transfer (FRET) was observed with the phthalocyanines used. The efficiency of FRET between the QDs and TtfmMPyZnPc and TtfmPyZnPc was found to be 0.31% and 0.45% in DMSO and 0.24% and 0.32% in pyridine, respectively. The triplet state quantum yields for TtfmMPyZnPc and TtfmPyZnPc were found to be 0.86 and 0.74 in DMSO and 0.83 and 0.76 in pyridine.

© 2009 Elsevier B.V. All rights reserved.

1. Introduction

Phthalocyanines (Pcs) are known as excellent functional materials. They have been studied in detail for many years, especially with regard to their properties as dyes and pigments. Chemical and physical studies of Pc compounds particularly those with substituents that enhance solubility of molecules, are pursued by chemists worldwide for their potential applications in many areas such as electrocatalysis [1–3], photocatalysis [4,5], electrochemistry [5], nonlinear optics [6], information storage [7], light emitting diodes [8], as liquid crystals [9,10], semiconductor materials [11] and as photosensitizers in photodynamic therapy of cancer [12,13]. Over the last decade, the photoactivity of numerous Pc based photosensitizers has been studied, with special focus on zinc, silicon and aluminium derivatives as a result of their desirable photophysical and photochemical properties [14].

However, because of the intermolecular interactions between the macrocycles, many Pc compounds are practically insoluble in common organic solvents, and thus the investigation on their properties and applications is restrained [15]. But, the solubility can be improved by introducing different kinds of solubility-enhancing substituents such as alkyl, alkoxyl and aryl groups on the periphery of the Pc ring [16–19]. Recently, fluorinated MPcs are receiving a great deal of attention [20–22]. Fluorinated phthalocyanines have been proven to have some advantages over non-fluorinated derivatives as photosensitizers for PDT [23,24].

Advances in research have led to the use of photosensitizers in combination with quantum dots (QDs) [25,26]. This arises from the excellent photophysical properties of QDs compared to organic dyes [27]. In addition to their high photostability, QDs can be size tuned resulting in different optical properties [27–29]. QDs are passivated to remove surface traps and hence increase their photostability thus maintaining their high photoluminescent nature. A variety of capping groups may be used to passivate the surface of QDs. Apart from serving the purpose of passivation, these capping groups also facilitate the interaction of QDs with their immediate environment [27]. The combined use of QDs and phthalocyanines usually results in Förster Resonance Energy Transfer (FRET) which is attributed to the non-radiative transfer of energy from a donor molecule to an acceptor molecule [30,31]. In this work the photophysical properties of the phthalocyanines **3** and **4** in the presence of QDs were studied. The molecules used in this study are: 4-(tetrakis-5-(trifluoromethyl)-2-mercaptopyridinephthalocyaninato) zinc(II) (TtfmMPyZnPc, **3**) and 4-(tetrakis-5 (trifluoromethyl)-2-pyridyloxyphthalocyaninato) zinc(II) (TtfmPyZnPc, **4**) (Scheme 1). The occurrence of FRET when Pcs are in the presence of QDs is now established [32–36]. However for water soluble positively charged Pcs containing aryl

* Corresponding author at: Rhodes University, Department of Chemistry, P.O. Box 94, Grahamstown, South Africa. Tel.: +27 46 6038260; fax: +27 46 6225109.
E-mail address: t.nyokong@ru.ac.za (T. Nyokong).

1010-6030/$ – see front matter © 2009 Elsevier B.V. All rights reserved.
doi:10.1016/j.jphotochem.2009.12.014

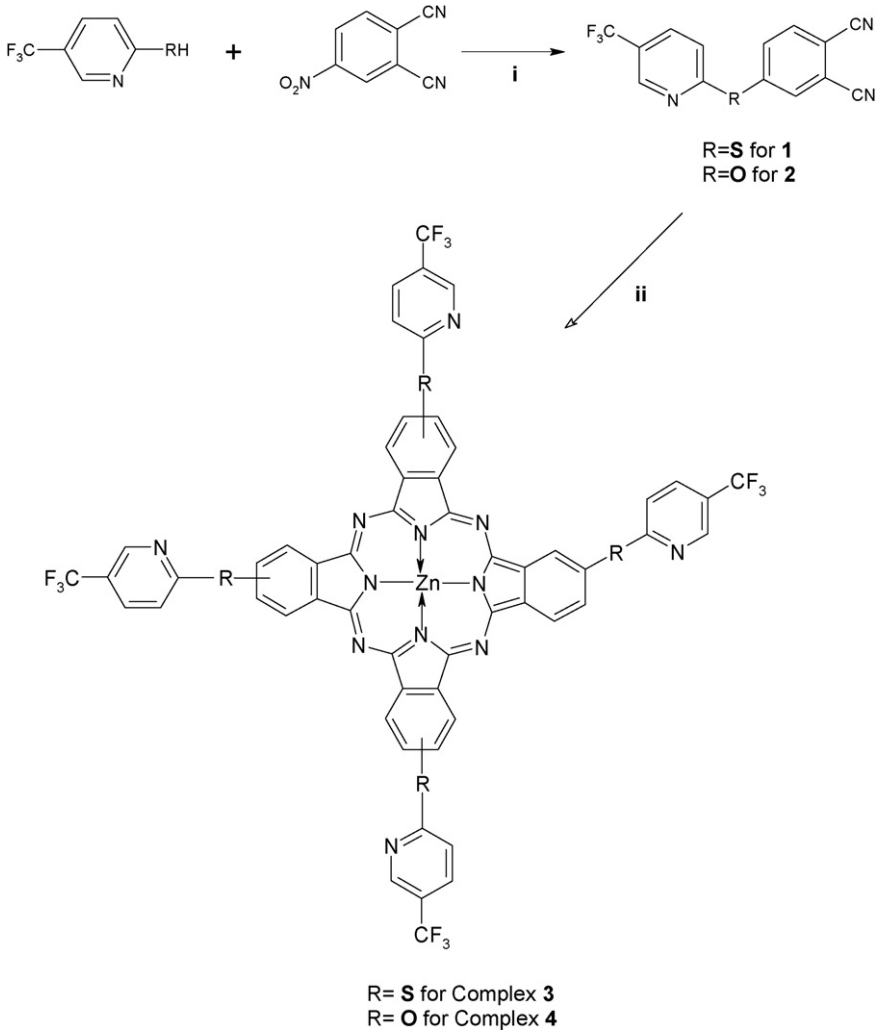

Scheme 1. Synthetic route of 4-[5-(trifluoromethyl)-2-mercaptopyridine]-phthalonitrile (**1**), 4-[5-(trifluoromethyl) pyridine]-phthalonitrile (**2**) and the respective zinc phthalocyanine derivatives (i) K_2CO_3, DMF, RT, 3 days (ii) anhydrous $Zn(Ac)_2$, pentanol, 12 h, 160 °C.

or alkyl thio substituents, interaction has been reported to result in aggregation and/or charge transfer [33]. The presence of a sulfur linkage in the aryl thio substituted Pc was found to result in aggregation in aqueous media, while when oxygen linkage was employed in aryl oxy substituted Pc aggregation was not observed. Hence in this work we compare the behaviours of complexes **3** (S linkage) and to **4** (O linkage) in the presence of QDs.

2. Experimental

2.1. Materials

3-Mercaptopropionic acid (MPA) 98%, tellurium powder (200 mesh, 99.8%), dimethyl sulfoxide (DMSO) and *N,N′*-dimethylformamide (DMF), chloroform ($CHCl_3$), tetrahydrofuran (THF), dichloromethane (DCM), methanol, pentanol, n-hexane, acetone and toluene were purchased from SAARCHEM; pyridine, zinc(II) phthalocyanine (ZnPc), cadmium chloride monohydrate ($CdCl_2{\cdot}H_2O$) and zinc acetate, 5-(trifluoromethyl)-2-mercaptopyridine, 2-hydroxy-5-(trifluoromethyl)pyridine, 1,2-diphenyl*iso*benzofuran (DPBF), 4-nitrophthalonitrile, 1,8-diazabicyclo[5.4.0] undec-7-ene (DBU) and potassium carbonate were purchased from Aldrich.

2.2. Characterization of quantum dots

3-Mercaptopropionic acid (MPA) capped QDs were synthesized according to reported methods [37]. The sizes of the QDs were determined using two different methods. These are X-ray powder diffraction (XRD), and fitting to a polynomial fitting function, Eq. (1) [38]:

$$D=(9.8127\times10^{-7})\lambda^3-(1.7147\times10^{-3})\lambda^2+(1.0064)\lambda-(194.84) \quad (1)$$

The fitting function is not valid for sizes for quantum dots outside the size range 1–9 nm [38]. The size was determined to be 4.24 nm using this equation.

2.3. Fluorescence quantum yield

Fluorescence quantum yields (Φ_F) were determined by a comparative method [39] using Eq. (2):

$$\Phi_F=\Phi_{F(Std)}\frac{FA_{Std}n^2}{F_{Std}An_{Std}^2} \quad (2)$$

where F and F_{Std} are the areas under the fluorescence curves of the ZnPc derivatives and the reference, respectively. A and A_{Std} are the absorbances of the sample and reference at the excitation wavelength, and n and n_{Std} are the refractive indices of solvents used for the sample and standard, respectively. ZnPc in DMSO was used as a standard, $\Phi_F = 0.20$ [40] for the determination of fluorescence quantum yields of the ZnPc derivatives. Rhodamine 6G in ethanol with $\Phi_F = 0.94$ was employed as the standard for the quantum dots [41,42]. The sample and the standard were both excited at the same relevant wavelength. $\Phi_{F(QD)}$ denotes the fluorescence quantum yields of the QDs where QD represents MPA capped CdTe QDs, and for the ZnPc derivatives the Φ_F values are represented as $\Phi_{F(ZnPc)}$ (where ZnPc represents TtfmMPyZnPc (**3**), and TtfmPyZnPc (**4**)). The determined fluorescence quantum yield values of the QDs were used to determine their fluorescence quantum yields in the mixture with ZnPc derivatives ($\Phi^{Mix}_{F(QD)}$) using Eq. (3):

$$\Phi^{Mix}_{F(QD)} = \Phi_{F(QD)} \frac{F^{Mix}_{QD}}{F_{QD}} \quad (3)$$

where F^{Mix}_{QD} is the fluorescence intensity of QDs in the mixture (with ZnPc derivatives) when excited at the excitation wavelength of the QDs (500 nm), F_{QD} is the fluorescence intensity of the QD alone at the same excitation wavelength and $\Phi_{F(QD)}$ was used as standard.

2.4. Triplet state quantum yields and lifetimes

Triplet quantum yields were determined using a comparative method, Eq. (4):

$$\Phi^{Sample}_T = \Phi^{Std}_T \frac{\Delta A^{Sample}_T \varepsilon^{Std}_T}{\Delta A^{Std}_T \varepsilon^{Sample}_T} \quad (4)$$

where ΔA^{Sample}_T and ΔA^{Std}_T are the changes in the triplet state absorbance of the ZnPc derivatives and the standard, respectively. ε^{Sample}_T and ε^{Std}_T are the triplet state extinction coefficients for the ZnPc derivatives and standard, respectively. Φ^{Std}_T is the triplet state quantum yield for unsubstituted zinc phthalocyanine (ZnPc) used as standard, $\Phi^{Std}_T = 0.65$ (in DMSO) [43] and $\Phi^{Std}_T = 0.65$ (in pyridine) [44]. Φ_T was also determined for the mixture of QDs and ZnPc derivatives and is represented as $\Phi^{Mix}_{T(ZnPc)}$ and the corresponding triplet lifetime as $\tau^{Mix}_{T(ZnPc)}$.

2.5. Determination of FRET parameters

Förster resonance energy transfer (FRET) is a nonradiative energy transfer from a photoexcited donor fluorophore to an acceptor fluorophore of a different species which is in close proximity, after absorption of a higher energy photon. FRET is dependent on a number of parameters including: the center-to-center separation distance between donor and acceptor (r), the degree of spectral overlap of the donor's fluorescence emission spectrum with the acceptor's absorption spectrum (J) [41,42]. FRET is evidenced by a decrease of the donor photoemission accompanied by an increase in the acceptor's fluorescence. The FRET efficiency (*Eff*) is determined experimentally from the fluorescence quantum yields of the donor in the absence ($\Phi_{F(QD)}$) and presence ($\Phi^{Mix}_{F(QD)}$) of the acceptor using Eq. (5) [41,42]:

$$Eff = 1 - \frac{\Phi^{Mix}_{F(QD)}}{\Phi_{F(QD)}} \quad (5)$$

FRET efficiency (*Eff*) is related to r (Å) by Eq. (6) [42]:

$$Eff = \frac{R_0^6}{R_0^6 + r^6} \quad (6)$$

where R_0 (the Förster distance, Å) is the critical distance between the donor and acceptor fluorophores at which the efficiency of energy transfer is 50%. R_0 depends on the quantum yield of the donor, Eq. (7) [42]:

$$R_0^6 = 8.8 \times 10^{23} \kappa^2 n^{-4} \Phi_{F(QD)} J \quad (7)$$

where n, is the refractive index of the medium; Φ_F, the fluorescence quantum yield of the donor in the absence of the acceptor; J is the Förster overlap integral and κ^2 is the dipole orientation factor. In this case, it is assumed that κ^2 is 2/3. This assumption is often made for donor–acceptor pairs in a liquid medium, since their dipole moments are considered to be isotropically oriented during the excited state lifetimes. The use of the isotropic dynamical average ($\kappa^2 = 2/3$) is more appropriate than the static isotropic average ($\kappa^2 = 0.476$) because the donor–acceptor pair is not in a rigid medium. FRET parameters were computed using the program PhotochemCAD [45]. J, the Förster overlap integral, is defined by Eq. (8):

$$J = \int f_{QD}(\lambda) \varepsilon_{ZnPc}(\lambda) \lambda^4 \partial\lambda \quad (8)$$

where f_{QD} is the normalized QD emission spectrum; and ε_{ZnPc}, the molar extinction coefficient of ZnPc derivatives. λ is the wavelength of the acceptor (at the Q band).

2.6. Equipment

Fluorescence excitation and emission spectra were recorded on a Varian Eclipse spectrofluorimeter. UV–visible spectra were recorded on a Varian 500 UV–Vis/NIR spectrophotometer. IR data was obtained by using the Perkin-Elmer spectrum 2000 FTIR spectrometer. ^{1}H NMR spectra were recorded using a Bruker AMX 400 MHz spectrometer. Elemental analysis was done using a Vario-Elementar Microcube ELII.

Laser flash photolysis experiments were performed with light pulses produced by a Quanta-Ray Nd:YAG laser providing 400 mJ, 90 ns pulses of laser light at 10 Hz, pumping a Lambda-Physik FL3002 dye (Pyridin 1 dye in methanol). Single pulse energy ranged from 2 to 7 mJ. The analysing beam source was from a Thermo Oriel xenon arc lamp, and a photomultiplier tube was used as a detector. Signals were recorded with a two-channel 300 MHz digital real-time oscilloscope (Tektronix TDS 3032C); the kinetic curves were averaged over 236 laser pulses. The triplet life times were determined by exponential fitting of the kinetic curves using the program OriginPro 7.5.

X-ray powder diffraction patterns were recorded on a Bruker D8, Discover equipped with a proportional counter, using Cu Kα radiation ($\lambda = 1.5405$ Å, nickel filter). Data were collected in the range from $2\theta = 5^\circ$ to 60°, scanning at 1° min^{-1} with a filter time-constant of 2.5 s per step and a slit width of 6.0 mm. Samples were placed on a silicon wafer slide. The X-ray diffraction data were treated using the freely available Eva (evaluation curve fitting) software. Baseline correction was performed on each diffraction pattern by subtracting a spline fitted to the curved background and the full width at half-maximum values used in this study were obtained from the fitted curves.

Fluorescence lifetimes were measured using a time correlated single photon counting setup (TCSPC) (FluoTime 200, Picoquant GmbH) with a light emitting diode and a linear polariser (PLS-500 with PDL 800-B, Picoquant GmbH, 497 nm, 10 MHz repetition rate). Fluorescence was detected under the magic angle with a Peltier cooled photomultiplier tube (PMT) (PMA-C 192-N-M, Picoquant GmbH) and integrated electronics (PicoHarp 300E, Picoquant GmbH). A monochromator with a spectral width of about 16 nm was used to select the required emission wavelength band. The response function of the system, which was measured with a scat-

tering Ludox solution (DuPont), had a full width at half maximum (FWHM) of about 950 ps. The ratio of stop to start pulses was kept low (below 0.05) to ensure good statistics. All luminescence decay curves were measured at the maximum of the emission peak. The data were analysed with the program FluoFit (Picoquant GmbH). The support plane approach was used to estimate the errors of the decay times.

2.7. Synthesis

2.7.1. 4-[5-(Trifluoromethyl)-2-mercaptopyridine]-phthalonitrile (**1**)

The 4-nitrophthalonitrile (0.97 g, 5.58 mmol) was dissolved in DMF (10 ml) under argon and 5-(trifluoromethyl)-2-mercaptopyridine (1.00 g, 5.58 mmol) was added. After stirring for 30 min at room temperature, finely ground anhydrous potassium carbonate (2.30 g, 16.7 mmol) was added in portions during 4 h with efficient stirring. The reaction mixture was stirred under argon atmosphere at room temperature for 3 days. Then the mixture was poured into 200 ml iced water, and the precipitate was filtered off, washed with water and then dried. The crude product was recrystallized from ethanol. Finally the pure product was dried in vacuum. Yield: 1.40 g (85%). IR spectrum (cm^{-1}): 3092, 3057 (Ar–CH), 2235 (C≡N), 1599 (C=C), 1581 (C=N), 1476, 1379 (C–F), 1330, 1247,1215, 1113, 1007, 939, 849, 742, 688 (C–S–C), 603. ^{1}H NMR ($CDCl_3$): δ = 8.71 (1H, s, Ar–H), 8.04 (1H,s, Ar–H), 7.94–7.82 (3H, m, Ar–H), 7.44 (d, J = 8.29 Hz, 1H, Ar–H) Mpt: 127 °C.

2.7.2. 4-[5-(Trifluoromethyl)-2-pyridyloxy]-phthalonitrile (**2**)

The synthesis of **2** was similar to that of **1**, except 2-hydroxy-5-(trifluoromethyl) pyridine (1.00 g, 6.13 mmol) instead of 5-(trifluoromethyl)-2-mercaptopyridine was employed. The amounts of the other reagents were: 4-nitrophthalonitrile, 1.06 g (6.13 mmol) and anhydrous potassium carbonate, 2.38 g (18.0 mmol).

Yield: 1.0 g (56%). IR spectrum (cm^{-1}): 3076, 3053 (Ar–CH), 2238 (C≡N), 1597 (C=C), 1578 (C=N), 1492, 1384 (C–F), 1336, 1250 (C–O–C), 1169, 1116, 1065, 917, 853, 774, 616. ^{1}H NMR ($CDCl_3$): δ = 8.02 (d, J = 8.37 Hz, 1H, Ar–H), 7.97 (1H, s, Ar–H), 7.88–7.85 (2H, m, Ar–H), 7.62–7.59 (1H, m, Ar–H), 6.81 (d, J = 9.79 Hz, 1H, Ar–H). Mpt: 222 °C.

2.7.3. 4-Tetrakis-(5-trifluoromethyl-2-mercaptopyridine) phthalocyaninato zinc(II) (**3**)

Compound **1** (0.40 g, 1.31 mmol), anhydrous zinc acetate (0.28 g, 1.31 mmol) and 2.5 ml of dry pentanol were placed in a standard Schlenk tube in the presence of 1,8-diazabicyclo [5.4.0] undec-7-ene (DBU) (0.31 ml, 0.20 mmol) under an argon atmosphere and held at reflux temperature for 12 h. After cooling to room temperature, the reaction mixture was precipitated by adding it drop-wise into n-hexane. The crude product was precipitated, collected by filtration and washed with hot hexane. The crude green product was further purified by a silica gel column using THF and then a mixture of $CHCl_3$:MeOH (100/5, v/v) as eluents. Yield: 140 mg (30%). UV–vis (DMSO): λ_{max} nm (log ε) 366 (4.75), 619 (4.55), 685 (5.21). IR spectrum (cm^{-1}): 3064 (Ar–CH), 1594 (C=C), 1574 (C=N), 1489, 1442, 1400, 1332 (C–F), 1326, 1247, 1074, 1009, 908, 830, 765, 743, 685 (C–S–C), 649 (Pc skeletal). ^{1}H NMR (DMSO-d6): δ = 8.65 (4H, s, Ar–H), 8.11–7.70 (16H, m, Ar–H), 7.34 (d, J = 8.18 Hz, 4H, Ar–H). Calcd for $C_{56}H_{24}F_{12}N_{12}S_4Zn$: C, 52.28; H, 1.88; N, 13.06; S, 9.97%. Found: C, 52.33; H, 2.21; N, 12.88; S, 10.51%. Mpt: >350 °C.

2.7.4. 4-Tetrakis-(5-trifluoromethyl-2-pyridyloxy) phthalocyaninato zinc(II) (**4**)

The synthesis of **4** was as outlined for **3**, except compound **2** (0.30 g, 1.04 mmol) instead of compound **1** was employed. The amounts of the other reagents were anhydrous zinc acetate (0.23 g, 1.04 mmol), dry pentanol (2 ml) and DBU (0.25 ml, 0.16 mmol) and the dark green product was obtained following purification. Yield: 85 mg (27%). UV–vis (DMSO): λ_{max} nm (log ε) 359 (4.82), 612 (4.60), 678 (5.28). IR spectrum (cm^{-1}): 3064 (Ar–CH), 1594 (C=C), 1571 (C=N) 1489, 1442, 1332 (C–F), 1292, 1061 (C–O–C), 923, 835, 751, 706, 630 (Pc skeletal). ^{1}H NMR (DMSO-d6): δ = 7.97–7.51 (21H, m, Ar–H), 7.03–6.99 (3H, b s, Ar–H). Calcd for $C_{56}H_{24}F_{12}N_{12}O_4Zn$: C, 55.03; H, 1.98; N, 13.75%. Found: C, 54.62; H, 2.12; N, 13.58%. Mpt: ≥350 °C.

3. Results and discussion

3.1. Synthesis and characterization

3.1.1. ZnPc derivatives

The synthetic procedure of new compounds is outlined in Scheme 1. The phthalonitrile derivatives: 4-[5-(trifluoromethyl)-2-mercaptopyridine]-phthalonitrile (**1**) and 4-[5-(trifluoromethyl)-2-pyridyloxy]-phthalonitrile (**2**) were obtained by base-catalyzed nucleophilic aromatic nitro displacement of 4-nitrophthalonitrile with the –SH and –OH functions of 5-(trifluoromethyl)-2-mercaptopyridine, or 2-hydroxy-5-(trifluoromethyl) pyridine, respectively (Scheme 1). The reactions were carried out at room temperature in anhydrous DMF with K_2CO_3 as a base.

The characteristic vibrations corresponding to CN at 2235 cm^{-1} (for **1**), 2238 cm^{-1} (for **2**), and C–S–C at 688 cm^{-1} (for **1**) and C–O–C at 1250 cm^{-1} (for **2**) were observed in the FTIR spectra. Aromatic C–H peaks were observed at above 3050 cm^{-1}. The ^{1}H NMR spectra of **1** and **2** showed signals at δ ranging from 7.44 to 8.71 for **1** and 6.81 to 8.02 for **2**, belonging to aromatic protons, integrating for 6 protons for **1** and **2** as expected.

Cyclotetramerization of **1** and **2** was carried out in the presence of anhydrous $Zn(OAc)_2$ in pentanol at reflux temperature under argon atmosphere. DBU was used as a strong base. The green cyclotetramerization complexes, ZnPcs, were purified by column chromatography and were obtained in moderate yields (30% for **3** and 27% for **4**). Elemental analysis results and the spectral data (^{1}H NMR, FTIR and UV–vis) of new compounds are consistent with the assigned formulations.

The cyclotetramerization of compounds **1** and **2** can be seen clearly by the absence of the CN peaks at 2235 and 2238 cm^{-1}, respectively, on the FTIR spectrum on formation of complexes **3** and **4**. The characteristic vibrations corresponding to C–S–C and C–O–C groups were observed at 685 cm^{-1} (for **3**) and 1061 cm^{-1} (for **4**), respectively, and aromatic C–H peaks, were above 3050 cm^{-1} for the complexes.

The ^{1}H NMR spectra of tetrasubstituted phthalocyanine derivatives (**3** and **4**) showed complex patterns due to the mixed isomer character of these compounds. The compounds were found to be pure by ^{1}H NMR with both the substituents and ring protons observed in their respective regions. In the ^{1}H NMR spectrum of **3** the aromatic and Pc protons appear between 8.65 and 7.34 ppm and for **4** between 7.97 and 6.99 ppm, integrating for a total of 24 protons for each complex. Elemental analysis results also were consistent with the proposed structures of **3** and **4** as expected. Attempts to quaternize the complexes were however unsuccessful.

3.1.2. Quantum dots

X-ray powder diffraction (XRPD) can provide information both about the crystal-structure and nanocrystalline properties of the QDs. Fig. 1 shows the X-ray diffraction patterns of the synthesized CdTe QD nanoparticles. The diffraction peaks are observed at 2θ = 25.2°, 41.6° and 48.9° to give the QD size of 4.54 nm using

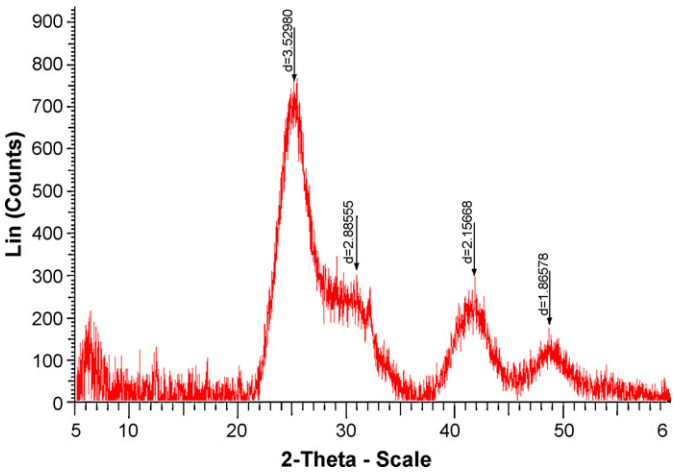

Fig. 1. X-ray diffractogram of mercaptopropionic acid stabilized CdTe quantum dots.

the in-built Scherrer equation (9):

$$d(\text{Å}) = \frac{k\lambda}{\beta \cos\theta} \tag{9}$$

where k is an empirical constant equal to 0.9, λ is the wavelength of the X-ray source (1.5405 Å), β is the full width at half maximum of the diffraction peak, and θ is the angular position of the peak. The QD size determined by this method was 4.54 nm, thus the sizes of QDs are in reasonable agreement with the particle-sizes obtained by polynomial fitting function (4.24 nm) (Eq. (1)) [38].

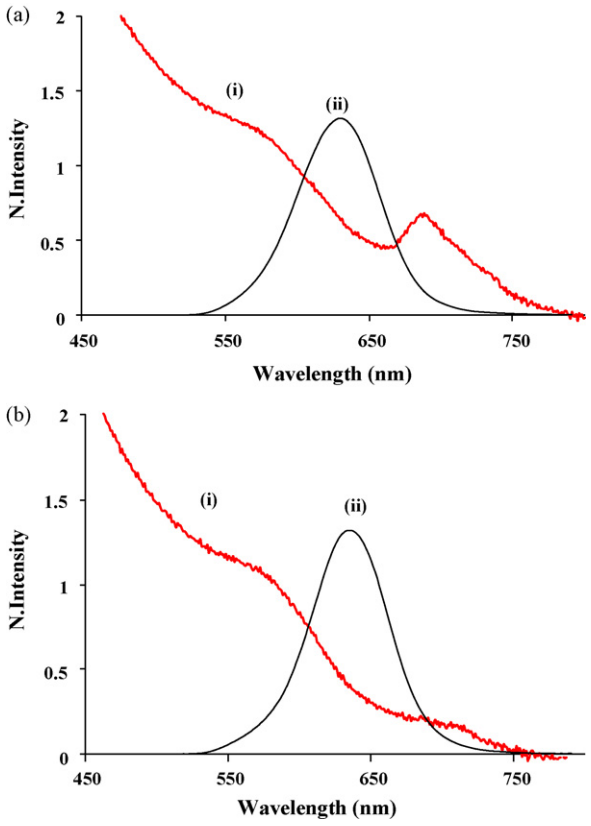

Fig. 2. Absorbance (i) and emission (ii) spectra of CdTe-MPA (0.2 mg/ml in (a) DMSO and (b) pyridine).

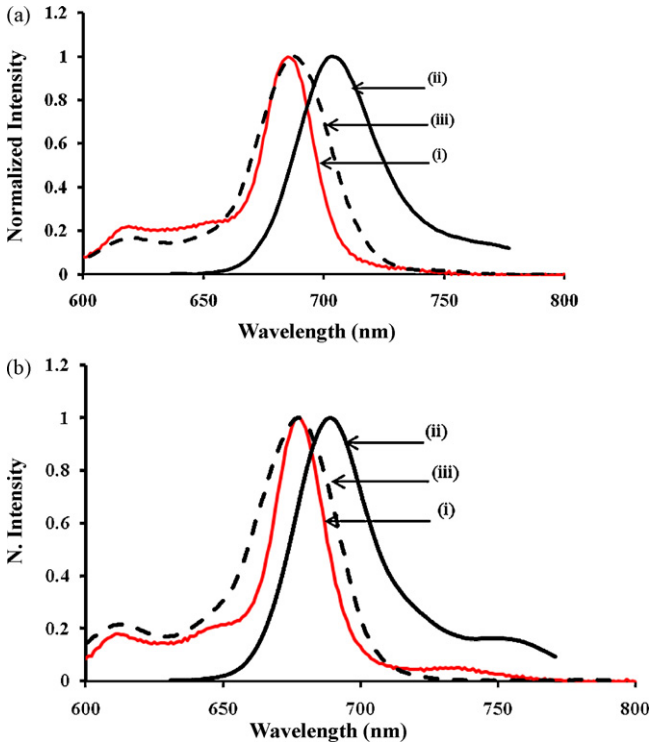

Fig. 3. Absorbance (i), emission (ii) and excitation (iii) spectra of TtfmMPyZnPc (**3**) (a) and TtfmPyZnPc (**4**) (b) in DMSO (excitation wavelength = 620 nm).

3.2. Ground state electronic absorption and fluorescence spectra

The ground state electronic absorption spectra of the MPA capped CdTe QDs in DMSO and pyridine (each containing < 1% water) is shown in Fig. 2. The absorption spectra of the QDs show typical [34] broad peaks in the visible region with tails extending to beyond 700 nm. The high photoluminescence which is typical of QDs, is evidenced in the emission spectra of these nanoparticles

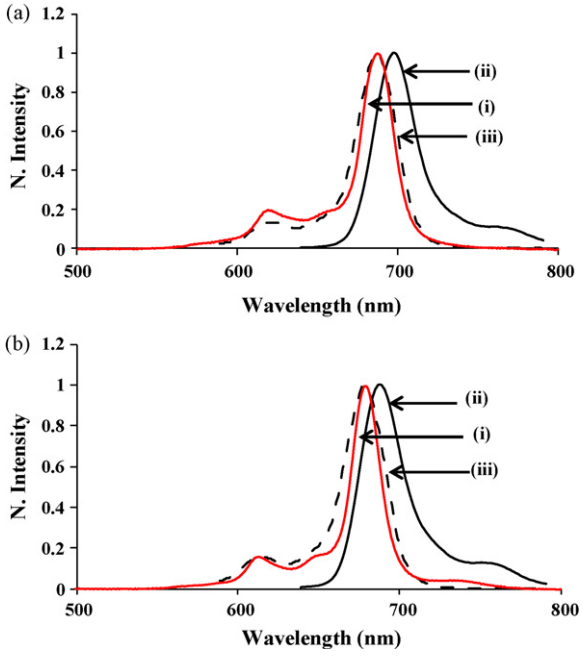

Fig. 4. Absorbance (i), emission (ii) and excitation (iii) spectra of TtfmMPyZnPc (a) and TtfmPyZnPc (b) in pyridine (excitation wavelength = 620 nm).

Table 1
Photophysical parameters for TtfmMPyZnPc and TtfmPyZnPc.

ZnPc	Solvent	Q band λ_{max} (nm)	Log ε	$\Phi_{F(ZnPc)}$ λ_{exc} (620 nm)[a]	$\Phi^{Mix}_{F(QD)}$ λ_{exc} (500 nm)[c]	$\Phi_{T(ZnPc)}$ [b]	$\tau_{T(ZnPc)}$ (μs)[b]
TtfmMPyZnPc (**3**)	DMSO	685	5.21	0.10	0.15 (0.22)	0.86 (0.88)	140 (263)
	Pyridine	685	5.27	0.17	0.1 (0.11)	0.83 (0.90)	4.60 (119)
TtfmPyZnPc (4)	DMSO	678	5.28	0.13	0.12 (0.22)	0.74 (0.88)	210 (262)
	Pyridine	678	5.24	0.18	0.1 (0.11)	0.76 (0.88)	11.3 (184)

[a] QDs size: CdTe-MPA = 4.54 nm.
[b] Values in brackets are for ZnPc derivatives in the presence of QDs.
[c] Values in brackets are for QDs alone.

Table 2
$\Phi_{F(QDs)}$ in various solvents.

Solvent	$\Phi_{F(QDs)}$
DMSO (1% water)	0.22
Pyridine (1% water)	0.11
DMF (1% water)	0.26
Water	0.35

(Fig. 2). The emission spectra are characterized by good symmetry and with a full width at half maximum (FWHM) of ~70 nm.

Fig. 3(a) and (b) shows the ground state electronic absorption spectra of TtfmMPyZnPc (**3**) and TtfmPyZnPc (**4**) in DMSO and Fig. 4(a) and (b) shows the spectra for both complexes in pyridine. TtfmMPyZnPc (**3**) and TtfmPyZnPc (**4**) show characteristic absorption in the Q-band region at 685 and 678 nm, respectively in DMSO and both complexes show monomeric behaviour in the solvents used. This monomeric behaviour is made evident by a single narrow Q band which is characteristic of metallated phthalocyanine complexes [46]. The Q-band position of TtfmMPyZnPc (**3**) is relatively red shifted in comparison to TtfmPyZnPc (**4**) (Table 1). This observation may be attributed to the presence of sulfur (S) atoms in the substituent groups of TtfmMPyZnPc (**3**) because these substituents are more e-donating than their oxygen linked counterparts by virtue of the S atoms [47]. The fluorescence spectra are mirror images of the excitation spectra which are similar to the absorption spectra of the complexes as shown in Figs. 3 and 4.

3.3. Photophysical and photochemical parameters

The Φ_F and Φ_T values for both ZnPc derivatives and QDs are listed in Table 1. The Φ_F values for the ZnPc derivatives are typical of MPc complexes [40]. These values are higher in pyridine when compared to DMSO (Table 1).

The Φ_F values for the QDs were also recorded in the DMSO, DMF, pyridine and water (Tables 1 and 2). The values are highest in water followed by DMF.

The values of Φ_T quantify the number absorbing molecules that undergo intersystem crossing to the triplet state. Φ_T and τ_T values attest to the efficiency of a phthalocyanine as a photosensitizer. The variation in Φ_T among the complexes depends on the heavy atom effect which encourages intersystem crossing to the triplet state. The observed trend for the Φ_T values corresponds well with the increase in atomic number of the substituents with TtfmMPyZnPc (**3**) having higher Φ_T than TtfmPyZnPc (**4**) by virtue of the sulfur atoms in complex **3**. The τ_T values ranged from 140 to 210 μs in DMSO which is within the usual range for Pcs and in pyridine they ranged from 5 to 11 μs (Table 1). Triplet lifetimes (τ_T) have been found to vary linearly with the logarithms of solvent viscosities for some MPc complexes [48]. This is observed in Table 1 where the less viscous pyridine shows shorter triplet lifetime values. An increase of the Φ_T and τ_T values in the presence of the quantum dots was observed for both phthalocyanines. The reason for this may be attributed to the heavy Cd and Te atoms which constitute the QDs and the result is that they encourage ISC of the MPc complexes. This should result in higher Φ_T and lower τ_T values. The enhancement of τ_T values in the presence of QDs has been previously reported by our group [32,49].

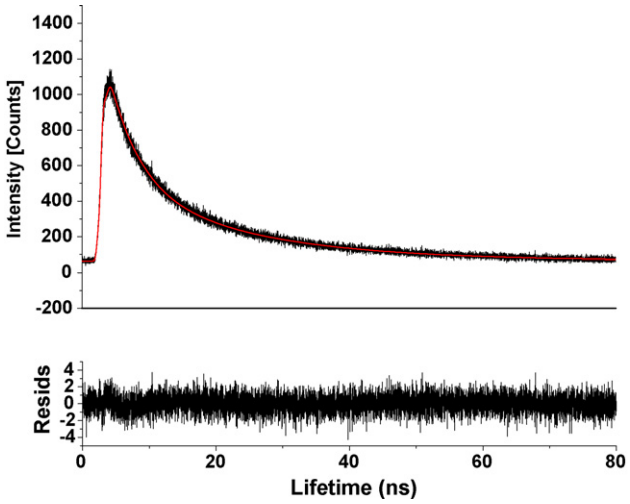

Fig. 5. Luminescence decay curve of MPA capped CdTe QDs in pyridine (λ_{ex} = 665 nm, measured at the maximum of the exciton emission peak, $\tau_{1/e}$ = 18 ns). Resids = residuals.

3.4. Interaction of ZnPc derivatives with QDs

3.4.1. Fluorescence lifetime studies

Table 3 shows the QDs fluorescence lifetime in the absence and presence of ZnPc derivatives, and Fig. 5 shows the luminescence

Table 3
Fluorescence lifetime measurements from interactions between TtfmMPyZnPc, TtfmPyZnPc and CdTe-MPA QDs (in pyridine and DMSO, each containing 1% water).

Sample	Solvent	τ_1 (ns)	τ_2 (ns)	α_1 [a]	α_2 [a]
MPA QD	Pyridine	4.0 ± 0.2	18.4 ± 0.2	0.53	0.47
MPA QD + **3**	Pyridine	3.3 ± 0.2	14.2 ± 0.5	0.66	0.34
MPA QD + **4**	Pyridine	3.1 ± 0.1	13.3 ± 0.3	0.63	0.37
MPA QD	DMSO	3.7 ± 0.7	34 ± 1.2	0.25	0.75
MPA QD + **3**	DMSO	3.8 ± 0.4	34.1 ± 1.5	0.35	0.65
MPA QD + **4**	DMSO	4.0 ± 0.5	33.3 ± 0.8	0.40	0.60

[a] α denotes the fraction of the amplitude.

Table 4
Variation of the binding and quenching constants of the TtfmMPyZnPc and TtfmPyZnPc complexes with CdTe-MPA QDs in DMSO and pyridine (each containing 1% water).

ZnPc	Solvent	k_q ($\times 10^{-13}$ M^{-1})	k_b ($\times 10^{-5}$M^{-1})	K_{SV} ($\times 10^{-5}$ M^{-1})	n
TtfmMPyZnPc (**3**)	DMSO	4.56	2.86	15.53	1.03
	Pyridine	8.15	0.53	14.95	0.90
TtfPyZnPc (**4**)	DMSO	1.75	1.68	5.99	1.06
	Pyridine	3.01	0.22	6.01	0.91

intensity decay of MPA QDs in pyridine. The data obtained from our time resolved luminescence measurements showed the QDs to have a two different emission decay times in both pyridine and DMSO (Table 3). The shorter lifetime is usually attributed to the excitonic recombination of the core states while the much longer lifetime usually involves the surface state carrier recombination processes [50]. The measurements taken in pyridine show reduction of the longer lifetime τ_2 of the QDs from 18 to 14 ns and 13 ns upon addition of complexes **3** and **4**, respectively indicating that the surface states are involved in the quenching process. The amplitude values give a measure of abundance of species with excitonic recombination within the core of the QD which compete with recombination from the surface states. A higher amplitude is an indication of a greater population of the particular species in solution. The results showed that in pyridine the QD lifetimes in both the absence and the presence of complexes **3** and **4** had a larger population of the QD species with recombination from the QD core states. The shorter lifetimes in pyridine were also slightly reduced in the presence of Pcs as can be seen from Table 3. In DMSO however there was no apparent quenching of the QDs fluorescence lifetime in the presence of the ZnPc derivatives for the competing excitonic recombination processes. QD species with recombination from the QD surface states were more predominant for studies in DMSO. The reason for the seeming lack of change in lifetime values in DMSO may be attributed to the very weak signal of the quenched QDs. The intensity of the signals was quite low as can be judged from Fig. 5. Since the solutions used were very dilute in an attempt to avoid reabsorption processes more counts would be needed to give signals of better intensity.

3.4.2. Binding constants and fluorescence quenching

Fig. 6 shows the fluorescence emission spectra of QDs at a known concentration of 0.1 mg/1 ml titrated with varying concentrations of the respective ZnPc derivative solutions (0–2.1 × 10^{-6} M). The QDs were excited at 500 nm and fluorescence recorded between 510 and 800 nm. The steady decrease in the fluorescence intensity of QDs with increase in ZnPc derivative concentration can be attributed to fluorescence quenching of the former. The changes in QD fluorescence emission intensities were related to the ZnPc derivative concentrations with the use of the Stern–Volmer relationship shown in Eq. (10) [51].

$$\frac{F_0}{F} = 1 + K_{SV}[\text{ZnPc}] \tag{10}$$

where K_{SV} represents the Stern–Volmer quenching constant, F_0 and F are the fluorescence intensities of the QDs in the absence and presence of ZnPc derivative, respectively. K_{SV} is given by Eq. (11):

$$K_{SV} = k_q \tau_F^{QD} \tag{11}$$

where k_q is the bimolecular quenching constant and τ_F^{QD} is the fluorescence lifetime of MPA capped CdTe QDs whose values are shown in Table 3 and were in agreement with known values for similar sized QDs [52].

Since the values of K_{SV} can be obtained from slopes of the plot of F_0/F versus [ZnPc] (ZnPc being derivatives **3** or **4**) then the value of k_q can be determined (Eqs. (10) and (11)). Fig. 6 has an inset that shows the Stern–Volmer plot indicating that the results are in agreement with the Stern–Volmer equation for the range of concentrations that were employed for this study. K_{SV} and k_q values are listed in Table 4.

In Fig. 7(a) and (b) the ground state absorption spectra show evidence for the formation of a ground state complex between the QDs and the ZnPc derivatives. This ground state complex (most likely formed by adsorption) is evidenced by the 2 nm shift of the Q-band positions of the complexes (**3**) and (**4**) upon addition of

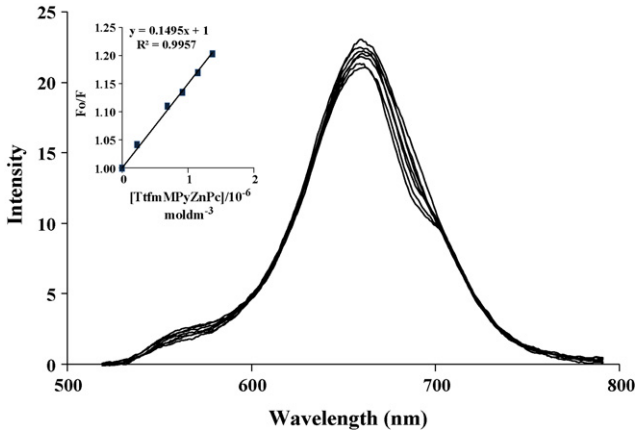

Fig. 6. Variation of the photoemission spectra of CdTe-MPA QDs (0.1 mg/ml) in the presence of varying concentrations (0–2.1 × 10^{-6} mol dm^{-3}) of the TtfmMPyZnPc (in pyridine). Inset: plot of [TtfmMPyZnPc] versus F_0/F.

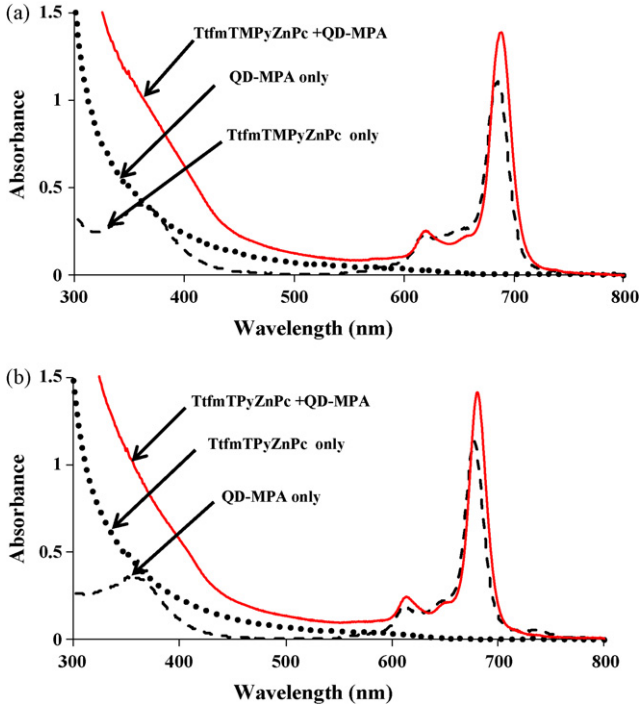

Fig. 7. Absorption of CdTe (MPA), ZnPc derivative alone and a mixture of ZnPc derivative and QDs, (a) TtfmMPyZnPc and (b) TtfmPyZnPc in DMSO.

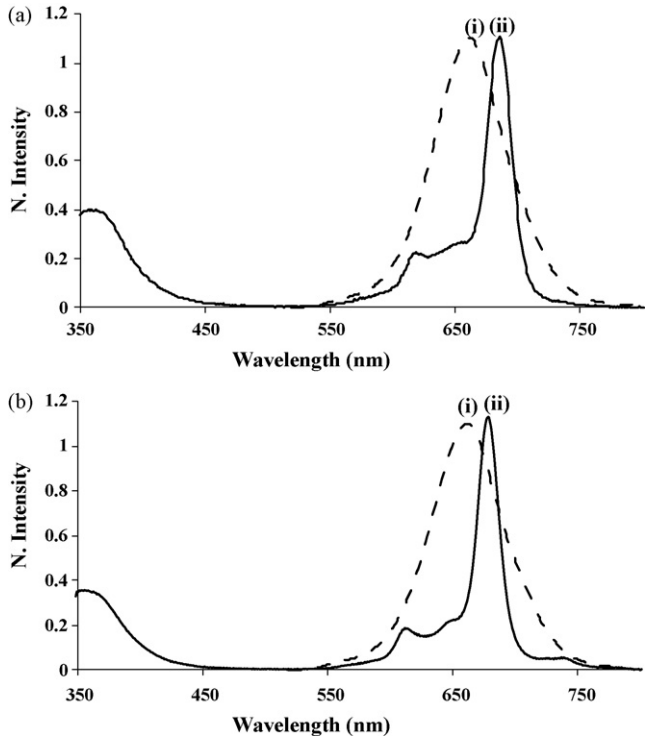

Fig. 8. Absorbance spectrum of ZnPc derivative (ii) and emission spectrum of CdTe (MPA) (i), (a) TtfmMPyZnPc and (b) TtfmPyZnPc in DMSO ($\lambda_{excitation}$ = 500 nm).

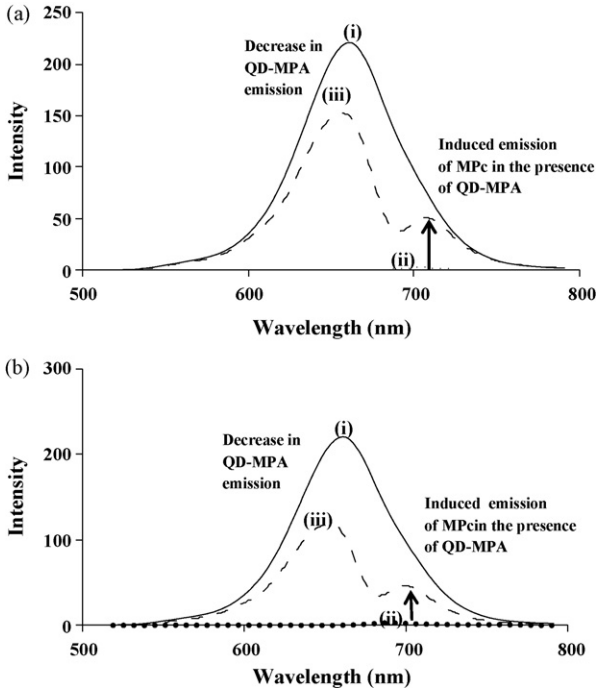

Fig. 9. Emission of (i) QDs alone (0.5 mg/ml), (ii) ZnPc derivative alone and (iii) QDs in the mixture with the ZnPc derivative (a) TtfmMPyZnPc (7.40×10^{-6} M) and (b) TtfmPyZnPc (6.30×10^{-6} M) ($\lambda_{excitation}$ = 500 nm, in DMSO).

the QDs to the ZnPc solutions. Thus, the determined K_{SV} values are static quenching constants due to the formation of the ground state complex by the QDs and the Pcs. The k_q values are of the order of 10^{13} dm^3 mol^{-1} s^{-1} (Table 4) which is higher than the proposed values for dynamic quenching which are of the order of 10^{10} dm^3 mol^{-1} s^{-1} [44]. This further indicates that the mode of quenching is static.

Fluorescence quenching experiment was then used to determine the binding constants (k_b) and the number of binding sites (n) by employing Eq. (12) [51,53,54]:

$$\log\left[\frac{(F_0 - F)}{F - F_\infty}\right] = \log k_b + n \log[\text{ZnPc}] \quad (13)$$

where F_0 and F are the fluorescence intensities of QDs in the absence and presence of ZnPc derivative, respectively; F_∞, the fluorescence intensity of QDs saturated with ZnPc derivative. Plots of $\log((F_0 - F)/(F - F_\infty))$ against log[ZnPc] provided the values of n (from slope) and k_b (from the intercept). The calculated k_b values were of the order of 10^5 suggesting strong interaction of the Pcs and QDs (Table 4). The value of n was found to be near unity, confirming that one ZnPc molecule interacts with the QDs as observed before [34].

3.4.3. Energy transfer

A large overlap was observed between the absorption spectra of complexes **3** and **4** with the MPA capped CdTe QDs (Fig. 8(a) and (b)) suggesting the possibility of efficient FRET. A decrease in the emission intensity of the QDs followed with the emergence of the emission peak of the respective Pc was observed in Fig. 9(a) and (b) upon excitation at 500 nm of a mixture containing the QDs and TtfmMPyZnPc and TtfmPyZnPc, respectively, where the ZnPc derivatives do not absorb. This observation suggests that non-radiative energy transfer takes place between the QDs and the Pc complexes. There was insignificant fluorescence emission for the ZnPcs upon excitation at 500 nm (Fig. 9(a) and (b) (curve ii)). The emergence of the Pc emission peaks in Fig. 9(a) and (b) (curve iii) was a result of FRET between the donor (QDs) and the acceptor (ZnPc) molecules.

Table 5 shows values of the overlap integral values (J) which are of the order of 10^{-12} cm^6. These values are relatively high when compared to values of the order 10^{-14} cm^6 which are typical for porphyrin based molecules [55]. Overlap integral values have varied units and in this work the units used were in cm^6 since the PhotochemCAD program gives J units in cm^6.

The center-to-center separation distance (r, Å) between donor and acceptor fluorophores was calculated using Eq. (6) and are listed in Table 5. The values of r were found to be greater than the values for the Förster distance, R_0 (Å) which is the critical distance between the donor and the acceptor molecule fluorophores for which efficiency of energy transfer is 50% [55,56]. As a result the energy transfer (*Eff*) was less than 50% for the ZnPc–QD mixtures. However the r values are still within the 2–10 nm range, thus

Table 5
Energy transfer parameters from interactions between TtfmMPyZnPc, TtfmPyZnPc and CdTe-MPA QDs (in pyridine and DMSO, each containing 1% water).

ZnPc	Solvent	J ($\times 10^{12}$ cm^6)	R_0 ($\times 10^{10}$ m)	r ($\times 10^{10}$ m)	*Eff*
TtfmMPyZnPc (**3**) + CdTe-QD (MPA)	DMSO	1.07	51.59	58.95	0.31
	Pyridine	1.15	59.44	72.03	0.24
TtfmPyZnPc (**4**) + CdTe-QD (MPA)	DMSO	1.17	52.15	53.56	0.45
	Pyridine	1.04	58.41	66.23	0.32

energy transfer is still possible if the fluorophores of the acceptor molecules are in close proximity to the fluorophores of the donor (QD's) molecules. It is expected that high *J* values and small *r* values will result in the highest efficiency of energy transfer (*Eff*). As shown in Table 5, TtfmPyZnPc in DMSO has highest *J* and smallest *r* value consequently it has the highest efficiency of energy transfer (*Eff*).

4. Conclusions

The photophysical properties of TtfmMPyZnPc and TtfmPyZnPc were studied in the presence of MPA capped CdTe QDs. A slight increase in the triplet state quantum yields and lifetimes was realized in the presence of QDs. This observation gives indication that there were increased diffusional interactions between the photosensitizer molecules and ground state molecular oxygen. Energy transfer was observed for both ZnPcs in the solvents used for these studies: dimethyl sulfoxide and pyridine. TtfmPyZnPc showed the highest efficiency of energy transfer in DMSO (*Eff* = 0.45).

Acknowledgements

This work was supported by the Department of Science and Technology (DST) and National Research Foundation (NRF), South Africa through DST/NRF South African Research Chairs Initiative for Professor of Medicinal Chemistry and Nanotechnology as well as Rhodes University. SM thanks DAAD foundation for a scholarship.

References

[1] J. Zagal, F. Bedioui, J.P. Dodelet (Eds.), N4-macrocyclic Metal Complexes, Springer, New York, 2006.
[2] K.I. Ozoemena, T. Nyokong, in: C.A. Grimes, E.C. Dickey, M.V. Pishko (Eds.), Encyclopedia of Sensors, vol. 3, American Scientific Publishers, California, 2006, p. 157 (Chapter E, and references therein).
[3] S. Griveau, J. Pavez, J.H. Zagal, J. Electroanal. Chem. 497 (2001) 75.
[4] P. Tau, T. Nyokong, J. Mol. Catal. A: Chem. 273 (2007) 149.
[5] D. Worhle, O. Suvorova, R. Gerdes, O. Bartels, L. Lapok, N. Baziakina, S. Makarov, A. Slodek, J. Porphyrins Phthalocyanines 8 (2004) 1020.
[6] M.F. Joseph, J.K. Thomas, V.E. Sven, J. Am. Chem. Soc. 121 (1999) 3453.
[7] W.S. Struve, J. Phys. Chem. B 103 (1999) 6835.
[8] G. De la torre, C.G. Claessens, T. Torres, Chem. Commun. (2007) 2000.
[9] N.B. McKeown, Chem. Ind. (1999) 92.
[10] M. Durmuş, S. Yeşilot, V. Ahsen, New J. Chem. 30 (2006) 675.
[11] M. Bouvet, in: K. Kadish, K.M. Smith, R. Guilard (Eds.), The Porphyrin Handbook, vol. 19, Academic Press, Boston, 2003, pp. 37–104.
[12] M.S. Wesley, E.V. Johan, M.A. Cynthia, Adv. Drug Deliv. Rev. 56 (2004) 53.
[13] M.W. Cecilia, H.S. Taroh, X. Liang-yan, H.G. Nahida, L.O. Nancy, Cancer Lett. 179 (2002) 43.
[14] H. Yanık, D. Aydın, M. Durmuş, V. Ahsen, J. Photochem. Photobiol. A: Chem. 206 (2009) 18.
[15] J. Rusanova, M. Pilkington, S. Decurtins, Chem. Commun. (2002) 2236.
[16] S. Banfi, E. Carous, L. Buccafurni, J. Organomet. Chem. 692 (2007) 1269.
[17] L. Guo, F.S. Meng, X.D. Gong, H.M. Xiao, K.C. Chen, H. Tian, Dyes Pigments 49 (2001) 83.
[18] L.D. Gao, X.H. Qian, J. Fluorine Chem. 113 (2002) 161.
[19] E.I. Yslas, V. Rivarola, E.N. Durantini, Bioorg. Med. Chem. 15 (2005) 39.
[20] M. Özer, A. Altindal, A.R. Özkaya, M. Bulut, Ö. Bekaroğlu, Polyhedron 25 (2006) 3593.
[21] T. Sugimori, M. Handa, K. Kasuga, Inorg. Chim. Acta 278 (1998) 253.
[22] E. Kol'tsov, I. Igumenov, T. Basova, P. Semyannikov, Mater. Chem. Phys. 86 (2004) 222.
[23] E.I. Yslas, E.N. Durantini, V. Rivarola, Bioorg. Medic. Chem. 15 (2007) 4651.
[24] K. Oda, S.I. Ogura, I. Okura, J. Photochem. Photobiol. B: Biol. 59 (2000) 20.
[25] S. Dayal, C. Burda, J. Am. Chem. Soc. 129 (2007) 7977.
[26] P. Juzenas, W. Chen, Y. Sun, M.A.N. Coelho, R. Generalov, N. Generalova, I.L. Christensen, Adv. Drug Deliv. Rev. 60 (2008) 1600.
[27] T. Jamieson, R. Bakhshi, D. Petrova, R. Pocock, M. Imani, A.M. Seifalian, Biomaterials 28 (2007) 4717.
[28] A.M. Smith, S. Nie, Analyst 129 (2004) 672.
[29] N. Gaponik, V.D. Talapin, K. Hoppe, E.V. Shevchenko, A. Kornowski, A. Eychmuller, H. Weller, J. Phys. Chem. B 106 (2002) 7177.
[30] L. Stryer, Annu. Rev. Biochem. 47 (1978) 819.
[31] L. Lankiewicz, J. Malicka, W. Wiczk, Acta Biochim. Pol. 44 (1997) 477.
[32] S. Moeno, T. Nyokong, Polyhedron 27 (2008) 1953.
[33] S. Moeno, T. Nyokong, J. Photochem. Photobiol. A: Chem. 201 (2009) 228.
[34] M. Idowu, J.-Y. Chen, T. Nyokong, New J. Chem. 32 (2008) 290.
[35] M. Idowu, T. Nyokong, J. Lumin. 129 (2009) 356.
[36] J. Britton, E. Antunes, T. Nyokong, Inorg. Chem. Commun. 12 (2009) 828.
[37] M. Idowu, E. Lamprecht, T. Nyokong, J. Photochem. Photobiol. A: Chem. 198 (2008) 7.
[38] W.W. Yu, L. Qu, W. Guo, X. Peng, Chem. Mater. 15 (2003) 2854.
[39] S. Fery-Forgues, D. Lavabre, J. Chem. Ed. 76 (1999) 1260.
[40] A. Ogunsipe, J.-Y. Chen, T. Nyokong, New J. Chem. 28 (2004) 822.
[41] R.F. Kubin, A.N. Fletcher, J. Lumin. 27 (1982) 455.
[42] J.R. Lakowiecz, Principles of Fluorescence Spectroscopy, 2nd edn., Kluwer Academic/Plenum Publishers, New York, 1999.
[43] P. Kubat, J. Mosinger, J. Photochem. Photobiol. A: Chem. 96 (1996) 93.
[44] S.L. Murov, I. Carmichael, G.L. Hug (Eds.), Handbook of Photochemistry, Marcel Dekker, Inc., New York, 1993.
[45] H. Du, R.A. Fuh, J. Li, L.A. Corkan, J.S. Lindsey, Photochem. Photobiol. 68 (1998) 141.
[46] M.J. Stillman, T. Nyokong, in: C.C. Leznoff, A.B.P. Lever (Eds.), Phthalocyanines: Properties and Applications, vol. 1, VCH Publishers, New York, 1989 (chapter 3).
[47] T. Nyokong, H. Isago, J. Porphyrins Phthalocyanines 8 (2004) 1083.
[48] A. Ogunsipe, M. Durmuş, D. Atilla, A.G. Gürek, V. Ahsen, T. Nyokong, Synth. Metals 158 (2008) 839.
[49] J. Ma, J.-Y. Chen, M. Idowu, T. Nyokong, J. Phys. Chem. B 112 (2008) 4465.
[50] X. Wang, L. Qu, J. Zhang, X. Peng, M. Xiao, Nanolett 3 (2003) 1103.
[51] D.M. Chipman, V. Grisaro, N. Sharon, J. Biol. Chem. 242 (1967) 4388.
[52] J. Ziang, R. Badugu, J.R. Lakowicz, Plasmonics 3 (2008) 11.
[53] S. Lehrer, G.D. Fashman, Biochem. Biophys. Res. Comm. 23 (1966) 133.
[54] S.M.T. Nunes, F.S. Sguilla, A.C. Tedesco, Braz. J. Med. Biol. Re. 37 (2004) 273.
[55] J.S. Hsiao, B.P. Krueger, R.W. Wagner, T.E. Johnson, J.K. Delaney, D.C. Mauzerall, G.R. Fleming, J.S. Lindsey, D.F. Bocian, R.J. Donohoe, J. Am. Chem. Soc. 118 (1996) 11181.
[56] T. Forster, Disc. Far. Soc. 27 (1959) 7.